第11回日本再生医療学会総会, 2012.6.13, パシフィコ横浜(神奈川)

5. 掛川貴弘、鈴木博章、福田淳二, 細胞脱離のための自己組織化オリゴペプチドの設計, 生物工学会第4回若手研究シンポジウム, 2012.7.1, モンタナリゾート岩沼（宮城県）
6. 掛川貴弘、Alfonso Gautieri、鈴木博章、福田淳二, 電気化学的細胞脱離のための自己組織化オリゴペプチドの設計, 日本バイオマテリアル学会シンポジウム2012, 2012.11.26, 仙台国際センター（宮城県）

G. 知的財産権の出願・登録状況

1. 特許取得

1) 福田淳二、鈴木博章、稲葉里奈、岡村健太郎、出願人：筑波大学、培養方法及び培養装置、特許第4911516号、出願2007.5.31、登録2012.1.27
Inventors: J Fukuda, H Suzuki, N Mochizuki, T Kakegawa、Applicants: University of Tsukuba、Cell culture method and device、International Application No.: PCT/JP2011/070533、International Filing Date: 8.9.2011

2. 実用新案登録

なし

3.その他

なし

別紙４

研究成果の刊行に関する一覧表レイアウト（参考）

書籍

著者氏名	論文タイトル名	書籍全体の編集者名	書　籍　名	出版社名	出版地	出版年	ページ
福田淳二	自己組織化単分子膜の電気化学的な脱離と再生医療への応用		Membrane	膜学会		2012	113-118
福田淳二	電気化学を用いた再生医療用培養皿の開発		バイオサイエンスとバイオインダストリー	バイオインダストリー協会		2012	142-143

雑誌

発表者氏名	論文タイトル名	発表誌名	巻号	ページ	出版年
N. Sadr, M. Zhu, T. Osaki, T. Kakegawa, Y. Yang, M. Moretti, J. Fukuda, A. Khademhosseini	SAM-based cell transfer to photopatterned hydrogels for microengineering vascular-like structures	*Biomaterials*	32(30)	7479-90	2011
J. Fukuda, Y. Kameoka, H. Suzuki	Spatio-temporal detachment of single cells using microarrayed transparent electrodes	*Biomaterials*	32(28)	6663-9	2011
N. Mochizuki, T. Kakegawa, T. Osaki, N. Sadr, N N. Kachouie, H. Suzuki, J. Fukuda	Tissue Engineering Based on Electrochemical Desorption of an RGD-Containing Oligopeptide	*Journal of Tissue Engineering and Regenerative Medicine*	7	236–243	2013
T. Kakegawa, N. Mochizuki, N. Sadr, H. Suzuki, J. Fukuda	Cell-adhesive and cell-repulsive zwitterionic oligopeptides for micropatterning and rapid electrochemical detachment of cells	*Tissue Engineering*	19(1-2)	290-8	2013

総説（Review Article）：膜（MEMBRANE），37（3），113-118（2012）

●特集　再生医療と膜学の接点

自己組織化単分子膜の電気化学的な脱離と再生医療への応用

福田淳二

筑波大学大学院　数理物質科学研究科
〒305-8573　茨城県つくば市天王台1-1-1

Electrochemical Desorption of Self-assembled Monolayers and Its Application for Regenerative Medicine

Junji Fukuda

Graduate School of Pure and Applied Sciences, University of Tsukuba
1-1-1, Tennoudai, 3F528, Tsukuba, Ibaraki 305-8573, Japan

Regenerative medicine aims to regenerate damaged tissues and organs by replacing them with tissue substitutes grown and reconstructed in the laboratory. One of the potential methods for reconstructing well-organized tissues *in vitro* is the use of cellular building blocks, such as cell sheets and spheroids. The fabrication and manipulation of such building blocks rely on innovative strategies for noninvasive cleavage of cell-to-culture substrate connections while preserving cell-to-cell connections. Several examples toward this end including our electrochemical approach have been presented. In our approach, cells are cultured on self-assembled monolayers (SAMs) of alkanethiols or oligopeptides adsorbed on a gold surface. The SAM was then reductively desorbed from the gold substrate by the application of a negative electrical potential. This caused the cells to detach from the gold surface in a rapid and reliable manner while maintaining cell-cell connections. This technology can be used to fabricate cell sheets, spheroids, and vascular-like structures.

Key words : self-assembled monolayer／electrochemistry／regenerative medicine／tissue engineering／cell sheet／spheroid

1. はじめに

再生医療とは細胞そのものを利用する新しい治療法であり，従来では治療できなかった患者を救命できる可能性があるため，大きな期待が寄せられている．特にこの分野は，日本発のiPS細胞作製技術の発見などもあり，近年国内でも注目が集まっている．ただし，たとえ免疫的に適合する細胞であっても，生体内へ単に細胞をインジェクションするだけでは，ごく一部の細胞しか生着せず十分な治療効果が得られないことが分かっている．つまり，iPS細胞などから必要な細胞が得られるようになるとしても，生体外であらかじめ組織体を構築する技術がなければ，より重要かつ複雑な臓器の再生医療は実現できない．

そこでこれまでに，耳や鼻などの比較的単純な組織は，生分解性多孔質ポリマーやハイドロゲルなどを必要な形状に加工し，これに細胞を播種して移植するアプローチが試みられてきた[1]．この方法は，すでに膀胱の再生医療などに臨床応用されている[2]．しかし，この方法は，移植後の細胞の増殖と自発的な組織化に大きく依存しており，生分解に伴う局所的なpHの低下など，いくつかの問題を抱えている．そのため，対象臓器によっては，細胞のみからなるよ

Tel: 029-853-5600 ext.8287（総研棟B322）
029-853-4995（第3学群F528）
Fax: 029-853-4490
E-mail: fukuda@ims.tsukuba.ac.jp

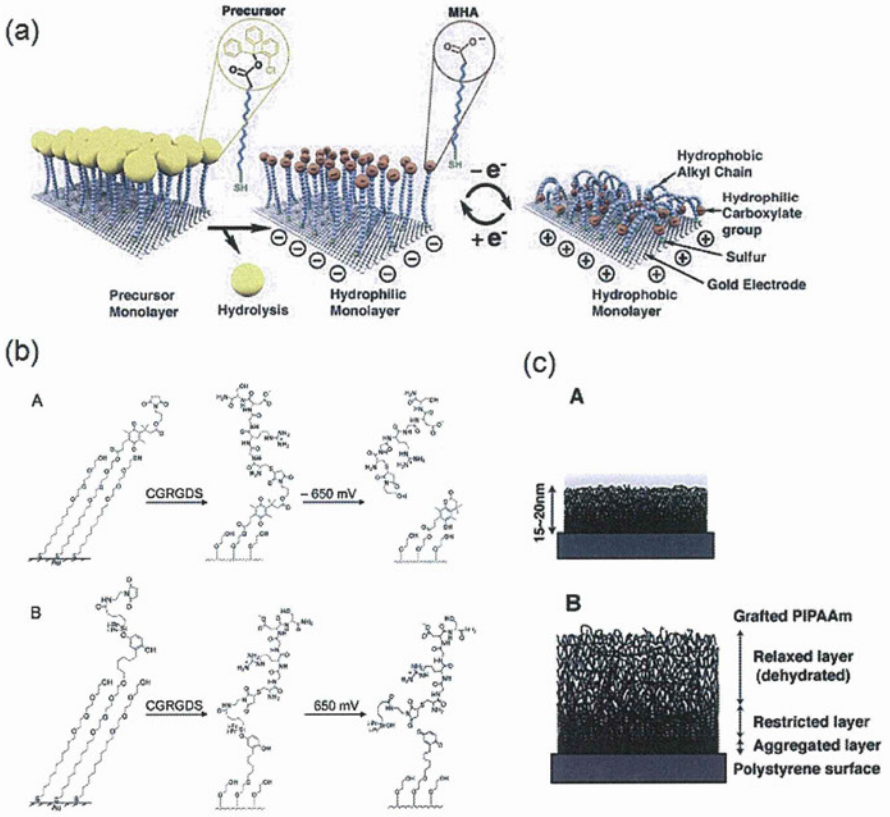

Fig. 1　Stimulus responsive film layers. (a) Electrically responsive monolayers[7]. (b) Electrically cleavable monolayer[8]. (c) Thermally responsive polymer film[16].

り生体組織に類似した組織体を作製する技術が求められている．例えば，伸縮が必要な心筋，透明性が必要な角膜，細胞同士の密な相互作用や立体構造が重要な肝臓や膵臓などでは，多孔質ポリマーを含まないアプローチがより適切と考えられる．

このような細胞のみの組織を構築するアプローチの1つとして，細胞シートや球状の細胞凝集体（スフェロイド）を作製し，これらをbuilding blocksとみなして適切に組み立てる方法論が提案されている[3]．文字通り，積み木やレゴの要領である．このようなアプローチを実現するためのキーテクノロジーとなるのが，外部刺激に応答して表面の性質を大きく変化させる「膜」である．つまり，細胞－細胞間の接着（組織構造）は維持したまま，細胞－培養表面間の接着のみを切断する機能性の分子膜が必要である．これまでに，単分子膜やポリマー薄膜を形成した培養表面などが報告されている．これらの膜は，厚みは数十nm，広さはcmオーダーという特徴的なサイズを持ち，電気，熱，光などに応答して膜構成分子のコンフォメーション変化を起こし，細胞を表面から脱離させるものである．本稿では，これら種々の刺激応答性膜コート表面と再生医療への応用について紹介する．

2.　刺激応答性分子膜

2.1　電気刺激

電気的な刺激を利用して表面の特性を大きく変化させるアプローチには，いくつか異なる手法がある[4〜6]．これらは，単分子膜の構造変化を利用するもの，電気化学的な反応を利用するものとに大別できる．前者は，例えばJ. Lahannらの報告している静電的な相互作用を利用する方法である（Fig. 1 (a)）．彼らは，嵩高いヘッドを持つアルカンチオール自己組織化単分子膜（self-assembled monolayer, SAM）を金表面に形成し，その後，ヘッドを除去することで低密度SAMを作製した．この分子膜では，電極表面に負電位を印加するとカルボキシル末端が表面に露出する（直立状態）．一方，正電位を印加するとカルボキシル末端が表面に引き寄せられアルキル鎖が表面に露出する．この変化により，表面の親水／疎水性およびインピーダンスをスイッチできることを報告している[7]．また後者には，例えばM. Mrksichらのグループの電気化学反応を利用する方法がある（Fig. 1 (b)）．彼らは，2種類のquinone類を含むSAMを利用し，それぞれが正または負の電位印加で

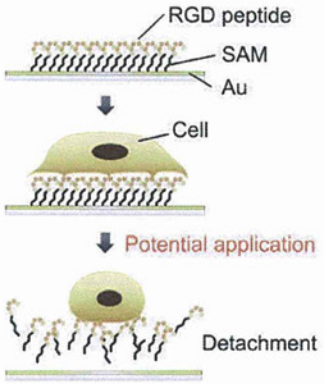

Fig. 2 Detachment of cells along with the electrochemical desorption of a SAM [18].

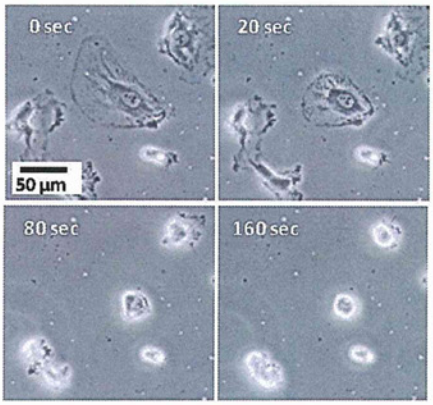

Fig. 3 Change in cell morphology after the application of the electrical potential.

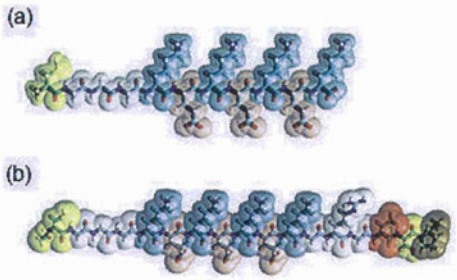

Fig. 4 Zwitterionic oligopeptides [19].

酸化または還元され，切断される反応を利用している[8]．これら以外にも電気化学反応によるpH変化を利用してポリイオンコンプレックス膜を解離させる方法などが報告されている[9]．

2.2 光刺激

光刺激に応答して分子構造を変化させ，表面の細胞接着性を変化させる方法も報告されている．これらのアプローチでは，azobenzenやspiropyranなど，光の波長に応じてシス-トランスの異性体変化を引き起こす分子を含む単分子膜が利用されている[10,11]．例えば，J. Auernheimerらは，中央にazobenzenを，片末端にRGDペプチドを備えた分子を用いている．この分子層で覆った表面に紫外光を照射することで，細胞の接着性を制御できることを示している[12]．また，A. Higuchiら[13]やJ. Edahiroら[14]は，spiropyranを利用して，同様に細胞の接着性を制御できることを報告している．光刺激を利用する利点は，高い空間分解能で表面の特性をスイッチできることである．

2.3 温度刺激

温度変化により表面の細胞接着性を制御する方法は，T. Okanoらのグループにより精力的な研究および臨床応用がなされている[15,16]．彼らは，Poly (N-isopropylacrylamide) のグラフト重合膜を利用して，細胞接着性を制御している．この膜は，37℃では細胞接着性であるものの，20℃程度に低下させると水和して細胞非付着性になるという特徴がある (Fig. 1 (c))．特に，細胞同士が二次元的に接着した細胞シートをこの表面で作製し，これを温度変化によって脱離・回収し，再生医療へ適用している．

3. 自己組織化単分子膜の還元脱離を利用した細胞脱離

3.1 細胞脱離

著者らは，上述した刺激応答性分子膜の中でも，電気刺激を利用したアプローチを検討してきた．刺激応答性分子膜を，空間分解能，時間分解能，可逆性の観点で比較すると，電気刺激を利用する方法は可逆性，空間分解能には劣るものの，時間分解能が高いと言える．なぜなら，電気刺激では，表面から数ナノメートルまでの局所的な領域に強力なエネルギー場を作ることができるためである[17]．これにより素早いスイッチングが期待できる．この電気化学エネルギーについて考えてみる．例えば，通常の化学反応では，熱運動によって活性化エネルギーの峠を越え反応が生じる．この熱運動エネルギーは温度Tの時は，$(3/2)RT$で表わされるため，仮に37℃とすると3.9 kJ/molに過ぎない．一方，1 Vの電圧は，電子1個のエネルギーで1 eV，よって97 kJ/molである．そして，語弊はあるものの $(3/2)RT$から逆にTに換算すると，7500℃もの高温に相当する．つまり，この局所的な強いエネルギーを表面反応，ここでは細胞脱離に，利用することで高い時間分解能が得られると考えられる．

著者らは，alkanethiol SAMを介して金電極表面に細胞を接着させ，gold–thiolate結合を電気化学的に切断することで，細胞を脱離させる手法を考案した (Fig. 2)[18]．この方法では細胞は培養表面から5分以内に脱離する (Fig. 3)．**2.3**に示した温度刺激による細胞脱離では30分～1時間を要するのと比較すると，素早い脱離法であると言える．

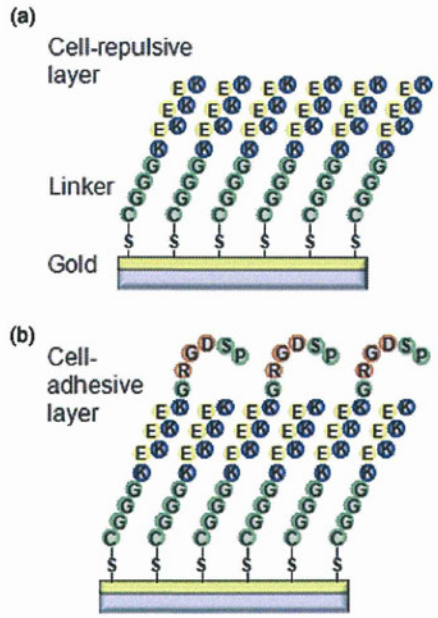

Fig. 5　Formation of self-assembled monolayers. Cell-repulsive (a) and adhesive (b) surfaces [19].

ところで，alkanethiolなどの分子は生体内に存在しないため，再生医療への応用を考えると，これらの分子の使用は将来の臨床応用において安全上の問題を引き起こす可能性がある．そこで，より生体適合性が高いと考えられるペプチドの利用を検討した[19]．つまり自己組織化能を有するオリゴペプチドをデザインし，電気化学細胞脱離への効果を検討した（Fig. 4）．このペプチドでは，片末端にチオール基を有するシステインを配置し，金表面との結合に用いる．中央にはポジティブおよびネガティブにチャージしたリジン（K）およびグルタミン酸（E）の繰り返し配列を導入し，金表面に末端を結合させた状態で，静電的な相互作用により密な分子層を形成するよう設計している（Figs. 4 (a)，5 (a)）．これまでの予備検討で，当該細胞脱離には，このようなタンパクの非特異吸着が生じない密な分子層の形成が重要であることが分かっている．さらに逆末端に細胞接着配列であるRGDを加えた細胞接着性のオリゴペプチドも設計した（Figs. 4 (b)，5 (b)）．この新しく設計したペプチドを用いて細胞脱離試験を行ったところ，alkanethiol SAMよりさらに短い，電位印加2分間でほぼすべての細胞が脱離することが示された（Fig. 6）．著者らの調べた範囲では，これまでにこのような短時間の細胞脱離は報告されていない．

3.2　オンデマンド細胞脱離

顕微鏡下で観察している興味ある特定の細胞を，その場で回収しオンデマンドに解析可能となれば，

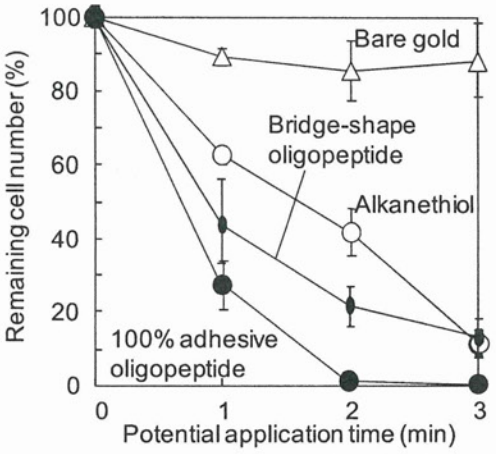

Fig. 6　Electrochemical cell detachment [19].

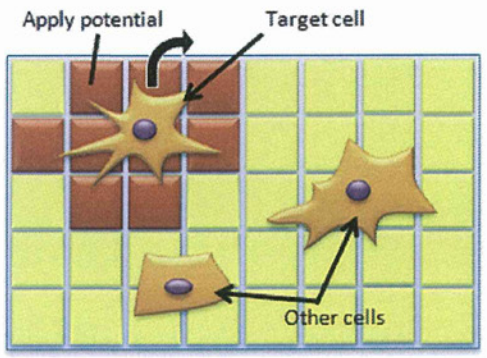

Fig. 7　Electrode arrays for selective cell detachment [20].

再生医療分野に限らず培養細胞を利用する様々な分野において有効なツールとなりうる．しかし，電気化学を利用した細胞脱離は，上述したように光を用いる場合と比較して空間分解能が低いと言える．つまり，光であれば，局所的に照射して細胞サイズ以下のスケールで細胞ー培養表面間の接着を切断することは容易であるが，この目的に電気刺激を利用するのは困難である．一方，光による細胞脱離には一般に紫外光が利用されるため，脱離させた細胞をさらに研究や医療応用する場合には適切とは言えない．

そこで空間分解能の高い電気化学的な細胞脱離法を確立するために，フォトリソグラフィーなどの微細加工技術を用いて，マイクロアレイ電極を作製した（Fig. 7）[20]．ただし，これまでのように金電極を利用すると，微小電極と電極間隙における光透過性の違いから，光学顕微鏡下ではハレーションが生じて電極上の細胞の観察が困難となる．そこで，透明電極として広く知られているITO電極（tin-doped indium oxide）を利用した微小電極アレイを作製した．すでに，ITO電極表面にalkanethiol SAMが形成されること，さらに負電位の印加によって表面から脱離

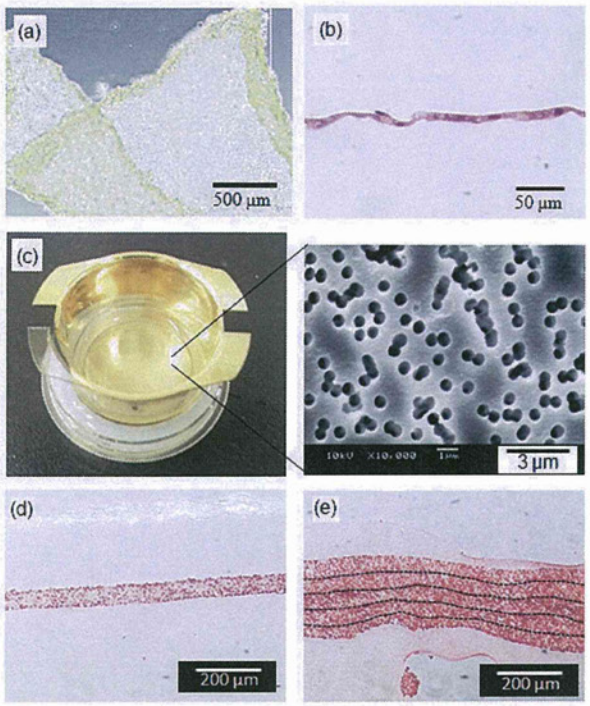

Fig. 8 Cell sheets formed on membrane substrates [18,22].

可能であることは報告されている[21]．我々は，接着細胞と同等スケールの微小電極をアレイし，5分間の電位印加でシングル細胞サイズの解像度で，特定の細胞を回収可能であることを示した．

3.3 細胞シートの脱離と積層化

上述した電気化学を用いた細胞脱離法は，二次元的に細胞同士が接着した細胞シートの脱離にも適用可能であった（Fig. 8 (a)）[18]．脱離させた細胞シートを別の細胞シートへ重ねて接着させ，再び脱離させるという操作を繰り返すことで，細胞シートを積層化することも可能であることを示した．ただし，細胞シートのサイズが大きくなるに従って，脱離に要する時間は延長する傾向が見られた．この一つの原因は，細胞シート自体が電気抵抗となり大きな電圧降下を引き起こしているためと考えられる．また，培養ディッシュ底面で細胞を重層化させた場合，簡単な拡散方程式から酸素不足が容易に生じることが導かれる[22]．

そこでこれらの状況を改善し，より大きくかつ厚みのある細胞シートを作製するために，多孔質膜に当該電気化学細胞脱離を応用した[23]．使用した多孔質膜はいわゆるトラックエッチング膜であり，400 nmの均一な孔が形成されている（Fig. 8 (c)）．この膜は，一般にセルインサートという名称で市販されており，細胞培養ディッシュ内に入れ，上下に培養培地を導入できるようになっている．これを利用することで，培地の気液界面から細胞培養面までの距離を短縮し，酸素供給速度を向上することができる．また，孔の存在によって細胞シートによる電気的抵抗の及ぼす影響を回避できると考えられる．実際にこの多孔質膜上では，細胞の増殖速度は向上し，14日間の培養で厚み50 μmの線維芽細胞シートが形成された（Fig. 8 (d)）．さらに，このシートを5枚積層化することで，ピンセットで操作できるほどの厚みのある細胞シートを作製することが可能であった（Fig. 8 (e)）．

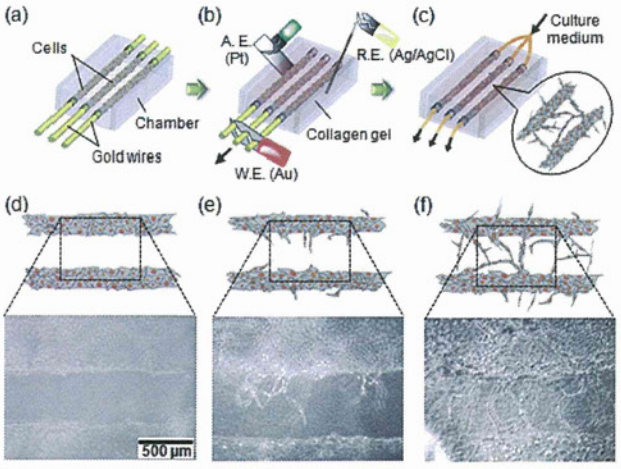

Fig. 9 Fabrication of capillary–like structures through the electrochemical cell detachment [22].

3.4 血管様構造作製への応用

上述したように細胞シートを積層化することで，厚みのある細胞シートが作製可能である．しかしながら，これ以上厚みを増加させると内部に壊死層が生じる．これは細胞組織内の酸素拡散を考えると当然のことであり，細胞シート表層を飽和酸素濃度に維持しても，生存限界厚みは，たかだか150～300 μm程度である．生体内の重要な臓器はいずれもcmオーダーであることを考えると，現状の技術レベルは，サイズにして何桁も低いと言える．生体外でmm～cmスケールの細胞組織・臓器を構築するには，送液可能な血管ネットワーク構造を構築する技術が必要である．

我々の電気化学細胞脱離技術は，平面のみならず円柱などの様々な形状に応用可能である．そこで，細胞脱離技術を金ロッドに適用し，コラーゲンゲルへ細胞を転写することで，内表面が血管内皮細胞に覆われた血管様構造を作製した（Fig. 9）[22,23]．血管内皮細胞は，適切な成長因子などの存在下で，コラーゲンゲル内において管腔構造を形成することが知られている（Fig. 9 (c)）．したがって，直径500 μm

の金ロッドを500 μm間隔で配置し，これ以下の血管ネットワーク構造の形成は細胞の管腔形成能に委ねるようにデバイスを設計した．このようなある程度荒い配置は，cmサイズへのスケールアップを考慮すると重要であると思われる．このデバイス内で14日間還流培養したところ，それぞれの血管様構造から伸長した管腔構造が互いに接続されることが示された（Fig. 9 (d) ～ (f)）．コラーゲンゲル内に増殖性の臓器幹細胞などをあらかじめ導入しておくことで，血管の伸長とともに組織化させ，送液可能な血管ネットワーク構造を備えた三次元組織を作製できるものと期待している．

5. おわりに

本稿では，単分子膜を形成した培養表面を利用した細胞接着性の制御技術とその再生医療への応用について解説した．特に著者らの単分子膜の電気化学的脱着反応を利用した細胞脱離技術について紹介した．ドナー不足のために治療できない患者に，自らの細胞を用いて移植可能な臓器を作り出す．これが再生医療の究極の目標である．そのためには，工学的なものづくり技術をますます取り入れる必要があり，中でも多孔質膜，単分子膜などの膜技術の果たす役割は非常に重要である．

文　献

1) Langer R and Vacanti JP : *Science*, **260**, (5110), 920-926 (1993)
2) Atala A, Bauer SB, Soker S, Yoo JJ, Retik AB : *Lancet*, **367**, 1241-1246 (2006)
3) Yamato M, Akiyama Y, Kobayashi J, Yang J, Kikuchi A, Okano T : *Prog. Polym. Sci.*, **32**, 1123 (2007)
4) Abbott NL, Gorman CB, Whitesides GM : *Langmuir*, **11**, 1, 16-18 (1995)
5) Chan EW, Park S, Yousaf MN : *Angew. Chem. Int. Ed.*, **47**, 33, 6267-6271 (2008)
6) Kim M, Lee JY, Shah S, Tae G, Revzin A : *Chem. Comm.*, **39**, 5865-5867 (2009)
7) Lahann J, Mitragotri S, Tran TN, Kaido H, Sundaram J, Choi IS, Hoffer S, Somorjai GA, Langer R : *Science*, **299**, (5605), 371-374 (2003)
8) Yeo WS, Mrksich M : *Langmuir*, **22**, 25, 10816-10820 (2006)
9) Guillaume–Gentil O, Akiyama Y, Schuler M, Tang C, Textor M, Yamato M, Okano T, and Vörös J : *Adv. Mater.*, **20**, 3, 560-565 (2008)
10) Ichimura K, Oh SK, Nakagawa M : *Science*, **288**, (5471), 1624-1626 (2000)
11) Hayashi G, Hagihara M, Dohno C, Nakatani K : *J. Am. Chem. Soc.*, **129**, 28, 8678-8679 (2007)
12) Auernheimer J, Dahmen C, Hersel U, Bausch A, Kessler H : *J. Am. Chem. Soc.*, **127**, 46, 16107-16110 (2005)
13) Higuchi A, Hamamura A, Shindo Y, Kitamura H, Yoon BO, Mori T, Uyama T, Umezawa A : *Biomacromolecules*, **5**, 1770-1774 (2004)
14) Edahiro J, Sumaru K, Tada Y, Ohi K, Takagi T, Kameda M, Shinbo T, Kanamori T, Yoshimi Y : *Biomacromolecules*, **6**, 970-974 (2005)
15) Yang J, Yamato M, Shimizu T, Sekine H, Ohashi K, Kanzaki M, Ohki T, Nishida K, Okano T : *Biomaterials*, **28**, 34, 5033-5043 (2007)
16) Matsuda N, Shimizu T, Yamato M, Okano T : *Adv. Mat.*, **19**, 20, 3089-3099 (2007)
17) 渡辺　正，金村聖志，益田秀樹，渡辺正義：「電気化学」，p.61，丸善株式会社（2005）
18) Inaba R, Khademhosseini A, Suzuki H, Fukuda J : *Biomaterials*, **30**, 21, 3573-3579 (2009)
19) Kakegawa T, Mochizuki N, Sadr N, Suzuki H, Fukuda J : *Tissue Eng.*, submitted.
20) Fukuda J, Kameoka Y, Suzuki H : *Biomaterials*, **32**, 28, 6663-6669 (2011)
21) Yan C, Zharnikov M, Golzhauser A, Grunze M : *Langmuir*, **16**, 15, 6208-6215 (2000)
22) Evenou F, Fujii T, Sakai Y : *Tissue Eng.*, **16**, 2, 311-318 (2010)
23) Mochizuki N, Kakegawa T, Osaki T, Sadr N, Kachouie NN, Suzuki H, Fukuda J : *J. Tissue Eng. Regen. M.*, Doi : 10.1002/term.519 (2012)
24) Seto Y, Inaba R, Okuyama T, Sassa F, Suzuki H, Fukuda J : *Biomaterials*, **31**, 2209-2215 (2010)
25) Sadr N, Zhu M, Osaki T, Kakegawa T, Yang Y, Moretti M, Fukuda J, Khademhosseini A : *Biomaterials*, **32**, 30, 7479-7490 (2011)

(Received 8 March 2012;
Accepted 11 March 2012)

著者略歴

福田　淳二（ふくだ　じゅんじ）

2003年3月　九州大学大学院工学府博士課程修了，博士（工学）
2003年4月　文部科学省知的クラスター創成事業　招聘研究員，北九州市立大学
2004年4月　日本学術振興会　特別研究員（PD）
2005年4月　Postdoctoral fellow, MIT, USA
2006年より現職

TOPICS

Culture dishes using electrochemistry for regenerative medicine

電気化学を用いた再生医療用培養皿の開発

福田淳二

キーワード　電気化学、自己組織化単分子膜、細胞シート、ティッシュ・エンジニアリング

はじめに

次世代の治療法として、再生医療への期待が高まっている。現在の医療技術では、重篤な患者を救命する最後の切り札は臓器移植である。しかし、移植には圧倒的なドナー不足という問題があり、また運よく移植を受けてもその後一生涯、免疫抑制剤を飲み続けなければならない問題がある。一方、再生医療では、患者自身の細胞から移植に利用できる臓器を作り出すことにより、これらの問題を解決できると考えられている。この分野では、患者の皮膚細胞などから万能性を持つ細胞（iPS細胞）を作り出す手法が、日本発の技術として近年発表され、脚光を浴びている。研究の進展は非常に早く、国内においても、すでに臨床試験の申請がなされている。また、再生医療は次世代大型産業としても注目されている。治療装置や培養器具なども含め、数年後には世界で数兆円規模に達すると予想されている。

1. 再生医療に用いる培養皿

免疫的に適合する細胞であっても、生体内へ単に細胞懸濁液を注入するだけでは、ごく一部の細胞しか生着せず、十分な治療効果が得られないことがよく知られている。つまり、万能細胞から必要な細胞が得られるとしても、生体外で組織・臓器を作製する技術が再生医療の実現には必要である。これまで、例えば耳や鼻などの組織は、生分解性多孔質ポリマーなどを必要な形状に加工し、これに細胞を播種して移植する方法が採られてきた。この方法は、すでに膀胱の再生医療などに臨床応用されている。ただし、移植後の細胞の増殖と自発的な組織化に依存するアプローチであり、生分解に伴って局所的にpHが低下したり、ポリマーの分解速度と細胞の増殖速度が釣り合わないなどの問題がある。そのため、対象臓器によっては、細胞のみからなるより生体類似の組織体を生体外で構築する技術が提案されている。例えば、伸縮が必要な心筋、透明性が必要な角膜などでは、多孔質ポリマーを含まない細胞のみからなる組織がより適切と考えられている。このアプローチの1つとして、温度応答性培養皿を用いた細胞シート技術がある。この培養皿は、細胞を増殖させてシート状態としたのちに、培養温度を20℃程度に低下させることで、細胞をシート状態のまま培養皿から剥離させることができるものである。この技術も日本発であり、すでに心筋の治療など臨床試験が実施され、新しい手法として注目されている。

2. 電気化学を利用した細胞シート作製

筆者らは、電気化学的な原理で細胞シートを作製する技術を近年報告した[1]。細胞シートを移植する際は、実は細胞シートは一層ではなく積層化したものを用いる。つまり、脱離させた細胞シートを別の細胞シートに重ね、さらに脱離させるという操作を複数回繰り返すことで、厚みのある積層化細胞シートを作製する。このとき、前述の温度応答性培養皿では1回の細胞脱離に30分以上を要するが、電気化学を利用する方法では約5分程度で脱離が可能であり、積層化に要する時間を短縮することができる。

この細胞脱離法の原理は、まずアルカンチオールまたはオリゴペプチド（図1）を金の表面に金－チオール結合で結合させ、自己組織化単分子膜を形成させる[2),3)]。そして、この分子層を介して細胞を接着させる。金電極に−1.0 V（vs. Ag/AgCl）の電位を印加することで金－チオール結合を切断し、このときの分子層の脱離に伴って細胞も脱離させるものである。実際に細胞脱離の様子を観察すると、細胞は周辺から脱離して次

筆者紹介：ふくだ・じゅんじ（FUKUDA, Junji）　筑波大学大学院数理物質科学研究科物性・分子工学専攻（Grad. Sch. of Pure and Appl. Sciences, Univ. of Tsukuba）講師　2003年九州大学大学院工学府博士後期課程修了　博士（工学）　専門：生物工学
連絡先：〒305-8573 茨城県つくば市天王台1-1-1　E-mail　fukuda@ims.tsukuba.ac.jp（勤務先）

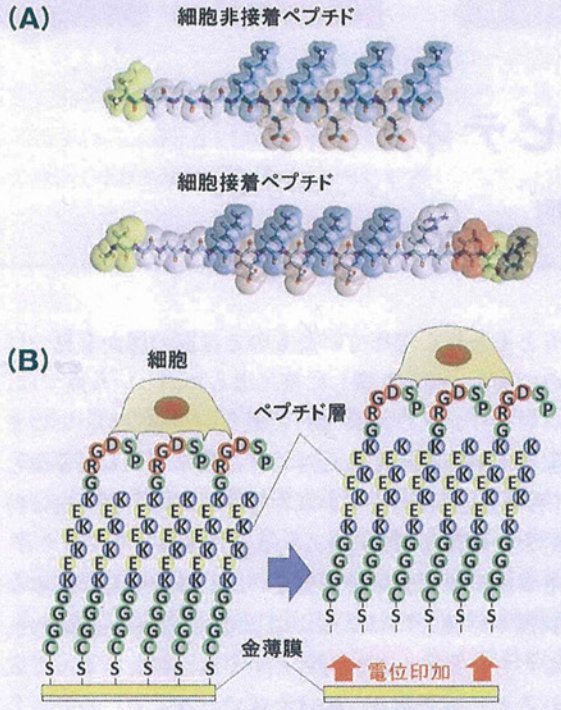

図1　電気化学的な細胞脱離の原理
(A) ペプチド　(B) 細胞脱離の模式図

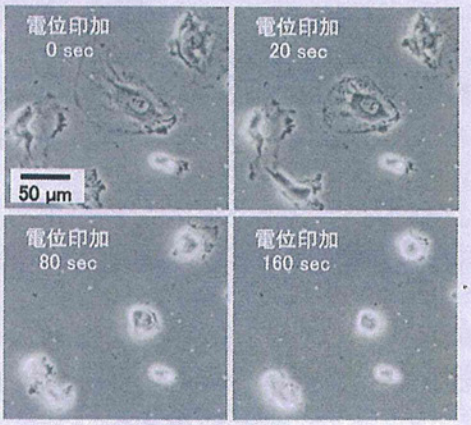

図2　細胞脱離の様子

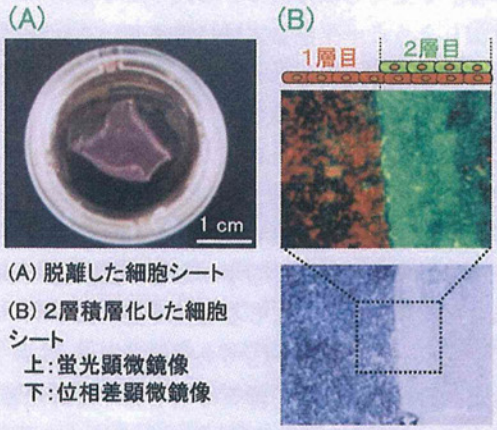

(A) 脱離した細胞シート
(B) 2層積層化した細胞シート
上：蛍光顕微鏡像
下：位相差顕微鏡像

図3　細胞脱離の様子

第に球形になり、シングル細胞の場合は現在のところ2～3分間でほぼすべての細胞を脱離可能である（図2）。また、脱離・回収した線維芽細胞を通常の培養皿に再び播種し、増殖速度を評価したところ、消化酵素（トリプシン）処理により脱離させた細胞とほぼ同じであることが示された。つまり、電気化学を用いる本手法は、細胞に大きな傷害を与えないことをすでに確認している。

基板上で線維芽細胞を増殖させシート状態としたあとに、電気化学的に脱離し別の線維芽細胞シートに積層化したところ、数時間以内の素早い細胞シート間の接着が観察された（図3）。組織染色の結果から、脱離させた細胞シートの下面には、細胞が培養中に分泌した細胞外マトリックスが蓄積していることがわかった。つまり、本手法では細胞脱離後にペプチド分子が細胞シート側に結合したままと考えられるが、細胞外マトリックスの蓄積のため、これが細胞シート間の接着を阻害しないことがわかった。

3.　今後の展望

ここで紹介した電気化学細胞脱離は、金をコートした基板をオリゴペプチド溶液中に浸漬するだけで培養表面が作製でき、また乾電池1本をこの培養基板に接続すれば素早い細胞脱離が得られるものである。したがって、電気的な特殊な装置や技術がなくとも幅広く利用できる安価な培養器具になり得る。今後、再生医療の発展を後押しする製品として、実用化も含めた検討を進めていきたい。

参　考　文　献

1) Inaba, R. *et al.* : Electrochemical desorption of self-assembled monolayers for engineering cellular tissues, *Biomaterials*, 30, 3573 ～ 3579 (2009)
2) Seto, Y. *et al.* : Engineering of capillary-like structures in tissue constructs by electrochemical detachment of cells, *ibid.*, 31, 2209 ～ 2215 (2010)
3) Sadr, N. *et al.* : SAM-based cell transfer to photopatterned hydrogels for microengineering vascular-like structures, *ibid.*, 32, 7479 ～ 7490 (2011)
4) Fukuda, J. *et al.* : Spatio-temporal detachment of single cells using microarrayed transparent electrodes, *ibid.*, 32, 6663 ～ 6669 (2011)

Biomaterials 32 (2011) 7479–7490

Contents lists available at ScienceDirect

Biomaterials

journal homepage: www.elsevier.com/locate/biomaterials

SAM-based cell transfer to photopatterned hydrogels for microengineering vascular-like structures

Nasser Sadr [a,b,c,d], Mojun Zhu [e], Tatsuya Osaki [f], Takahiro Kakegawa [f], Yunzhi Yang [g], Matteo Moretti [h], Junji Fukuda [a,f,*], Ali Khademhosseini [a,b,c,**]

[a] Center for Biomedical Engineering, Department of Medicine, Brigham and Women's Hospital, Harvard Medical School, Cambridge, MA 02139, USA
[b] Harvard-MIT Division of Health Sciences and Technology, Massachusetts Institute of Technology, Cambridge, MA 02139, USA
[c] Wyss Institute for Biologically Inspired Engineering, Harvard University, Cambridge, MA 02139, USA
[d] Bioengineering Department, Politecnico di Milano, 20131 Milan, Italy
[e] Department of Biology, Mount Holyoke College, South Hadley, MA 01075, USA
[f] Graduate School of Pure and Applied Sciences, University of Tsukuba, 1-1-1 Tennodai, Tsukuba, Ibaraki 305-8573, Japan
[g] Department of Restorative Dentistry and Biomaterials, University of Texas Health Science Center, Houston, TX 77030, USA
[h] Cell and Tissue Engineering Laboratory, IRCCS Istituto Ortopedico Galeazzi, 20161 Milan, Italy

ARTICLE INFO

Article history:
Received 1 June 2011
Accepted 14 June 2011
Available online 29 July 2011

Keywords:
Photocrosslinkable hydrogel
Zwitterionic oligopeptide
Electrochemical cell detachment
Gelatin methacrylate
Vascular microengineering
Endothelial monolayer

ABSTRACT

A major challenge in tissue engineering is to reproduce the native 3D microvascular architecture fundamental for *in vivo* functions. Current approaches still lack a network of perfusable vessels with native 3D structural organization. Here we present a new method combining self-assembled monolayer (SAM)-based cell transfer and gelatin methacrylate hydrogel photopatterning techniques for microengineering vascular structures. Human umbilical vein cell (HUVEC) transfer from oligopeptide SAM-coated surfaces to the hydrogel revealed two SAM desorption mechanisms: photoinduced and electrochemically triggered. The former, occurs concomitantly to hydrogel photocrosslinking, and resulted in efficient (>97%) monolayer transfer. The latter, prompted by additional potential application, preserved cell morphology and maintained high transfer efficiency of VE-cadherin positive monolayers over longer culture periods. This approach was also applied to transfer HUVECs to 3D geometrically defined vascular-like structures in hydrogels, which were then maintained in perfusion culture for 15 days. As a step toward more complex constructs, a cell-laden hydrogel layer was photopatterned around the endothelialized channel to mimic the vascular smooth muscle structure of distal arterioles. This study shows that the coupling of the SAM-based cell transfer and hydrogel photocrosslinking could potentially open up new avenues in engineering more complex, vascularized tissue constructs for regenerative medicine and tissue engineering applications.

1. Introduction

A major challenge in engineering functional tissues *in vitro* is to mimic the underlying *in vivo* 3D microarchitecture. Vasculature represents an outstanding example of complex spatially organized cellular/ECM structures, and their successful generation *in vitro* is known to be crucial for a range of applications such as regenerative medicine and drug discovery [1].

Self-organization of endothelial cells on 2D or within 3D biological gels is by far the most common approach to promote vascularization and angiogenetic processes in engineered tissues [2]. However, the extensive culture time needed to allow for cell migration and organization, the lack of control on 3D tubular organization, along with the limitations in attaining perfusable vessels *in vitro*, have so far hindered a successful transfer of this approach to tissue engineering applications.

These constraints have prompted the exploration of alternative approaches, often relying on microengineering techniques to fabricate vascularized tissue constructs. For instance the modular assembly of micrometric organoids covered with endothelial cells

* Corresponding author. Graduate School of Pure and Applied Sciences, University of Tsukuba, 1-1-1 Tennodai, Tsukuba, Ibaraki 305-8573, Japan.
** Corresponding author. Center for Biomedical Engineering, Department of Medicine, Brigham and Women's Hospital, Harvard Medical School, 65 Landsdowne Street, Cambridge, MA 02139, USA.
E-mail addresses: fukuda@ims.tsukuba.ac.jp (J. Fukuda), alik@rics.bwh.harvard.edu (A. Khademhosseini).

0142-9612/$ – see front matter © 2011 Elsevier Ltd. All rights reserved.
doi:10.1016/j.biomaterials.2011.06.034

has been shown to enable blood perfusion [3]. More recently, engineered perfusable microvessels were generated by seeding endothelial cells in microfluidic collagen gels and then successfully adopted to investigate the role of cyclic AMP in vascular barrier regulation [4]. However, seeding-based approaches can often be characterized by complex procedures or rely on several days of culture to form an endothelial monolayer [5]. Applying bioprinting principles, Norotte and colleagues fabricated hollow vascular structures by substituting cell seeding with the precise deposition of micron-sized cellular cylinders around an agarose molding template [6]. These approaches, which rely on complex and expensive instrumentation, so far have not been applied to the generation of vascular constructs lined with endothelial cell monolayer. Nonetheless, an *in vivo*-like endothelial monolayer would be critical to recapitulate native blood vessel functions such as the regulation of diffusion and extravasation processes.

As an alternative approach, we have recently demonstrated the generation of vascular-like structures by transfer of endothelial monolayers from gold rods to the internal surfaces of micrometric collagen channels [7]. This microengineering approach uses culture substrates modified with self-assembled monolayers (SAMs) of alkanethiol or oligopeptides that mediate cell detachment once electrochemically desorbed [8,9]. Cells can then be deposited on a receiving substrate with an approach similar to thermoresponsive polymer-based cell sheet engineering [10].

Here we studied the integration of zwitterionic oligopeptide SAM-based cell deposition with the photoinduced hydrogel crosslinking process. Hydrogels, indeed, provide a flexible microfabrication platform that can be applied to the generation of geometrically defined three dimensional (3D) constructs [11,12] and microfluidic channels [13]. In addition, due to the rapid hydrogel crosslinking, photoactivated approaches offer the advantage of minimized processing time. This is a critical parameter while engineering thick tissues with a high number of metabolically active cells that would benefit from the immediate onset of perfusion culture. More specifically, here we have adopted a previously developed gelatin methacrylate hydrogel, that has been shown to be cell adhesive and support proliferation of cells seeded on the surface and of those encapsulated within the gel [14]. We first investigated mechanisms responsible for the SAM-based cell detachment in transfer of single cells and monolayers from gold to hydrogel. The association of the SAM-based cell deposition and hydrogel photocrosslinking was further applied to the generation of micrometric single and double vascular structures.

2. Materials and methods

2.1. Materials and reagents

Glass slides (24 mm × 24 mm; No. 4) from Matsunami Glass (Japan), glass rods (diameter, 600 μm; length, 3.2 cm) from Hirschmann Laborgeräte (Germany), and synthetic oligopeptide, CGGGKEKEKEKGRGDSP, from Sigma–Aldrich (Japan) were used to fabricate culture substrates. Endothelial basal medium-2 (EBM-2, CC-3156) and SingleQuots growth supplement (CC-3162) from Lonza (Switzerland) were used for cell culture. Gelatin (Type A, 300 bloom, from porcine skin) and methacrylic anhydride were purchased from Sigma–Aldrich (USA) for methacrylated gelatin (GelMA) synthesis. Irgacure 2959 photoinitiator (2-hydroxy-1-(4-(hydroxyethoxy) phenyl)-2-methyl-1-propanone, CIBA Chemicals) was initiated by an ultraviolet (UV) light source (Omnicure S2000) from EXFO Photonic Solutions Inc. (Canada) for polymer photocrosslinking. All other chemicals were purchased from Sigma–Aldrich (USA) unless otherwise indicated.

2.2. Methacrylated gelatin synthesis and prepolymer solution preparation

GelMA was synthesized as previously described [14–16]. Briefly, type A porcine skin gelatin was added (10% w/v) to Dulbecco's phosphate buffered saline (PBS; GIBCO, USA), heated at 60 °C, and stirred for 1 h. Methacrylic anhydride was added (7.5% v/v) at a rate of 0.5 ml/min to the gelatin solution at 50 °C while stirring and allowed to react for 2 h. Samples were then dialyzed in 12–14 kDa cutoff dialysis tubing in distilled water at 40 °C for 1 week before being filtered (0.2 μm). Finally, the solution was frozen overnight (−80 °C), lyophilized for 1 week, and stored at −80 °C until further use.

A prewarmed (60 °C) 0.05% (w/v) photoinitiator (PI) solution in PBS (with Ca Mg) was mixed with GelMA macromers (5% w/v) until fully dissolved and was used when cooled to room temperature. Fresh prepolymer solution was prepared for each experiment.

2.3. Peptide design and gold surface modification

Gold substrates were prepared by sputter coating Cr (1 nm layer) and Au (40 nm layer) on glass slides and glass rods, which were pre-cleaned with ammonia/peroxide mix ($NH_4OH/H_2O_2/H_2O$, 1/1/4) [7,9]. The oligopeptide (CGGGKEKE-KEKGRGDSP) consists of three main functional domains, designed to generate SAMs on gold that prevent non-specific protein adsorption while exclusively mediate cell adhesion. On one end of the oligopeptide, cysteine has a thiol group that adsorbs to gold surface via a gold–thiolate (S-Au) bond (Fig. 1A). The central domain, composed of charged glutamic acid (E) and lysine (K) residues, promotes electrostatic packing of adjacent peptides, which enhances the non-fouling properties [17] of SAM. On the other end, the RGD motif mediates cell adhesion by interacting with integrins expressed on cell surface. Peptide adsorption does not require any organic chemistry and was obtained by incubating gold substrates in 5 μM aqueous oligopeptide solution at 4 °C for 16 h. Before cell seeding, the substrates were rinsed twice with pure water, once in 70% ethanol, and twice in PBS.

2.4. Cell culture

Immortalized human umbilical vein endothelial cells (HUVECs; a generous gift from Dr. J. Folkman, Children's Hospital, Boston) constitutively expressing green fluorescent protein (GFP) were cultured in EBM-2 supplemented with SingleQuots growth supplement. NIH 3T3 fibroblasts were cultured in Dulbecco's modified Eagle medium (Gibco, USA) supplemented with 10% fetal bovine serum (Gibco, USA) and 1% Penicillin/Streptomycin (Gibco, USA). All cells were cultured in standard cell culture incubators (5% CO_2, 37 °C). Culture medium was changed every 48 h, and cells were passaged when 60–70% confluence was reached.

2.5. Self-assembled monolayer stability

To evaluate SAM stability in a solution containing PI when exposed to UV (PI&UV), mass adsorption/desorption experiments and surface chemical characterization were performed. A Quartz Crystal Microbalance (QCM; Q-sense E4, Biolin Scientific/Q-Sense, Sweden) equipped with open measuring modules and gold coated sensors was used to measure the resonant frequencies of bare gold in double distilled water (ddH_2O). After incubation in the oligopeptide solution (5 μM) at 24 °C for 3 h, the sensors were rinsed with ddH_2O before measuring the resonant frequencies. Sensors were then exposed to PI&UV (0.05% w/v; 50 s, 6.5 mW/cm^2) and rinsed in ddH_2O before the final measurement.

Modified gold substrates were analyzed with X-ray photoelectron spectroscopy after PI&UV exposure. They were compared to those that were simply immersed in PBS. Samples were rinsed with ddH_2O and dried under N_2 before being analyzed by the spectrometer. X-ray photoelectron spectra were recorded using a Kratos AXIS Ultra spectrometer (Kratos Analytical Ltd, UK) with charge neutralizer. Oxygen (O1s), carbon (C1s), nitrogen (N1s), and gold (Au4f) spectra were obtained with a monochromatic Al Kα X-ray source (1486.6 eV) and pass energy of 20.0 eV. All spectra were calibrated with reference to Au4f at a binding energy of 83.65 eV. Spectra were obtained with similar settings (number of sweeps, integration times, etc.) for each sample and normalized to the Au 4f peak.

To investigate cell adhesion on gold substrates in the presence of PI&UV, HUVECs were seeded at a density of 7.5 × 10^4 cells/ml (2-ml for each well, 15.6 × 10^3 cells/cm^2) on gold coated glass slides modified with the oligopeptide. After 16-h incubation in a 5% CO_2 incubator at 37 °C, non-adherent cells were removed by aspirating the medium and rinsing in PBS (with Ca Mg). The samples were then immersed in PI solution (0.05% w/v) and exposed to UV for 50 s (6.5 mW/cm^2). Following irradiation, the samples were rinsed with PBS (with Ca Mg). Phase-contrast images of the gold surface were taken immediately before and after the procedure to investigate cell detachment and morphology. Non-modified gold substrates (with and without PI and UV) and modified substrates (without PI and UV, immersed in PBS) were adopted as controls.

2.6. Two dimensional cell transfer

Oligopeptide modified gold substrates were seeded with HUVECs (15.6 × 10^3 cells/cm^2) and incubated for 16 h. After rinsing samples in PBS (with Ca Mg), the GelMA prepolymer solution (800 μl) was poured onto the surface (confined by a polydimethylsiloxane, PDMS, mold 18 × 18 mm) and UV photocrosslinked for 50 s (6.5 mW/cm^2). Samples were then immersed in PBS (with Ca Mg) either with or without −1.0 V potential application (potentiostat, model 1100, Fuso Mfg. Co., Japan) for 2 min (Fig. 1B), followed by hydrogel layer removal from the substrate. Samples without oligopeptide modification were adopted as controls.

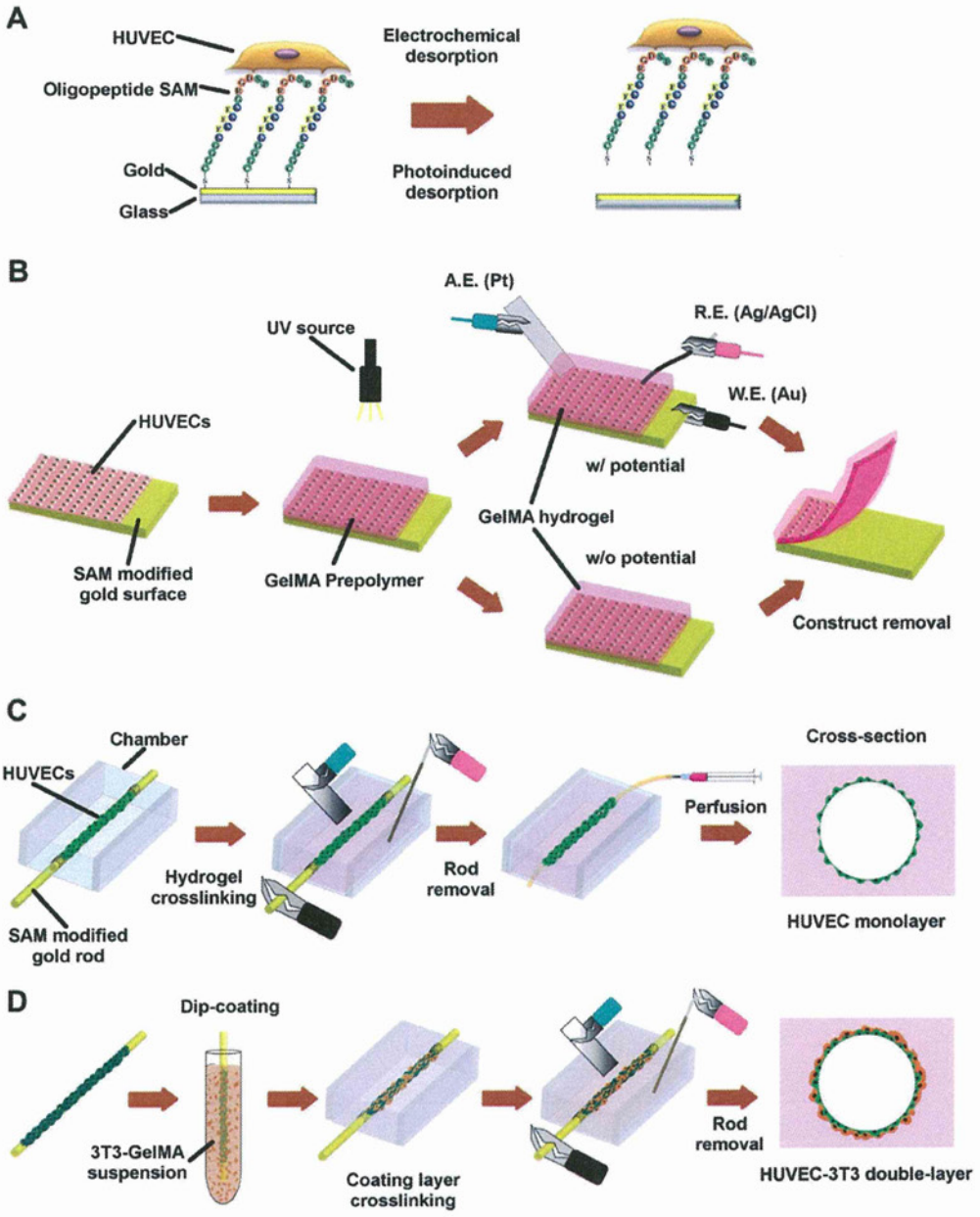

Fig. 1. Cell transfer and vascular construct generation schematic. (A) The oligopeptide CGGGKEKEKEKGRGDSP was chemically adsorbed onto a gold surface and seeded with HUVECs. SAM desorption from the surface resulted in cell detachment. (B) HUVECs seeded on gold substrates modified with oligopeptide based-SAM were transferred to the hydrogel after GelMA prepolymer photocrosslinking with or without electrical potential. (C) Micrometric gold rods enveloped with cells were positioned in culture chambers that were then filled with GelMA. After photocrosslinking, an electrical potential was applied and the endothelial cells were transferred. Following rod removal, the device was connected to a microsyringe pump and cultured under perfusion. (D) Double-layer cell microvascular structures were generated by dip-coating the gold rods enveloped with HUVECs in a GelMA solution containing 3T3 cells. The double-layered rods were then encapsulated in the hydrogel, cells were transferred by electrical potential application to the gel and the rod was removed. (For interpretation of the references to colour in this figure legend, the reader is referred to the web version of this article.)

Phase-contrast images at five different fields on the gold surface (immediately before and after cell transfer) and the hydrogel surface (immediately after each transfer) were acquired (MetaMorph®, Molecular Devices Inc., USA) by means of an inverted microscope (Axio Observer Z1, Carl Zeiss MicroImaging Inc., USA) equipped with a Cool Snap HQ^2 camera (Photometrics, USA) and a 10× lens (EC Plan-Neofluar 10×/0.3, Carl Zeiss MicroImaging Inc., USA). The number of cells per field of view was determined using the NIH ImageJ software. Transfer efficiency was expressed as a percentage of mean cell density on the hydrogel after cell transfer over the mean cell density on the corresponding gold surface before cell transfer.

Images of fluorescent GFP cells on gold (before cell transfer) and hydrogel (after cell transfer) were acquired (same settings) and employed to quantify individual cell area using ImageJ. The total number of cells evaluated was 691 for non-modified gold and 549 for gold coated with the peptide. On hydrogels, the total number of cells evaluated to calculate the cell area was 36 for hydrogel transferred from non-modified gold, while for modified gold it was respectively 707 for hydrogel transferred without and 1121 for those with potential.

Cell viability 2 h after transfer to the hydrogel was investigated with ethidium homodimer-1 (EthD-1) staining (LIVE/DEAD®, Molecular Probes®, USA). Fluorescent images were acquired with both GFP and DS-RED filter cubes. Merged images were used to quantify cell viability as the percentage of EthD-1 negative cells over total number of cells.

Cell proliferation and long term viability of samples transferred with and without potential, from oligopeptide modified substrates, were evaluated for up to 72 h after cell transfer. Phase images were acquired at 0, 12, 24, 48 and 72 h. The

number of cells per surface area was calculated at each time point and the percentage of spreading population was computed at 12 h. After 72 h, samples were stained with EthD-1 and the cell viability was calculated.

Experiments were run in triplicate for each condition.

2.7. Cell monolayer transfer

To evaluate the transfer efficiency for cell monolayer rather than single cells, gold coated glass slides modified with the oligopeptide were seeded either as described previously and cultured for 72 h, or at a high density (5×10^5 cells/ml, 2-ml for each well) and cultured for 16 h. After rinsing in PBS (with Ca Mg), the confluent cell layers were transferred either with or without potential application. Phase images were acquired before and after cell transfer and used to quantify cell transfer efficiency.

To evaluate the effect of cell transfer process on cell–cell junctions, cellular monolayers on gold substrates and on hydrogels (incubated 2 h in media after transfer), were fixed in paraformaldehyde (4%, 7 min) and immunostained with primary antibodies for VE-Cadherin (VE-Cad rabbit anti-human, Cayman Chemical Company, USA) or Connexin 43 (Cx43; rabbit anti-human, Abcam Inc, USA) and fluorophore conjugated secondary antibody (Cy5 goat anti-rabbit, Abcam Inc, USA), and counterstained with DAPI. All the experiments described above were run in triplicate for each experimental group. Images were taken with a confocal microscope (Leica SP5 X MP, Leica Microsystems, Wetzlar, Germany).

2.8. Microvascular structure generation

HUVECs were seeded on gold rods, modified with the oligopeptide as described for the gold slides, at a density of 1.5×10^5 cells/ml (6 ml for each petri dish) in ultra-low attachment 60 mm dishes (Corning, USA). The culture medium was changed after 24 h to remove excess cells and then every 48 h until confluence (3–4 days).

The chamber for perfusion culture ($2.5 \times 10 \times 10$ mm inner dimensions) was fabricated with poly(methyl methacrylate) (PMMA) plates using computer-aided laser machining (Laser PRO C180; GCC, Taiwan). To generate microvascular structures, gold rods with confluent cell layers were placed in the chamber, 250 μl of prepolymer solution dispensed in the chamber, and UV photocrosslinked for 50 s (6.5 mW/cm^2). Following hydrogel formation, the rods were extracted after potential application (−1.0 V, 5 min). Chambers were then connected to a microsyringe pump and perfused with medium at 2 μL/min (Fig. 1C).

Phase-contrast and fluorescent images of the construct were taken with an inverted microscope. The entire construct was visualized 12 h after cell transfer with a confocal microscope. After 15 days in culture, cell-laden hydrogels were fixed in paraformaldehyde (4%, 20 min) stained with DAPI and analyzed with an inverted microscope.

To generate complex 3D vascular structures double-layer cell microvascular structures were fabricated (Fig. 1D). In particular, NIH 3T3-fibroblasts that were stained with PKH26 red fluorescent membrane labeling (Sigma–Aldrich) were resuspended in GelMA solution (4×10^7 cells/ml) and then cooled to 18 °C to induce partial gelation. Modified gold rods with HUVEC monolayer were dipped in prepolymer solution, placed in the chamber, and photocrosslinked for 40 s (6.5 mW/cm^2). The chamber was then filled with prepolymer solution and UV photocrosslinked for 50 s. Fluorescent images of the construct were taken with an inverted microscope after the first photocrosslinking step. Cross-sectional images of the finished construct were taken with a confocal microscope and a 10× lens.

2.9. Statistics

Statistical significance was determined for replicates of 3 by an independent Student *t*-test for two groups of data or analysis of variance (ANOVA) followed by Bonferroni's post-hoc test for multiple comparisons using SigmaStat 3.0 (Systat Software, USA). Differences were considered significant for $p < 0.05$.

3. Results and discussion

3.1. Effect of photoinitiator and UV on self-assembled monolayer

Hydrogel photocrosslinking relies on UV induced radical formation of photoinitiator molecules [18], that initiates the formation of a polymer network [19,20]. However, besides electrochemical desorption, thiolate SAM removal from metal substrates can occur when the substrate is exposed to UV irradiation [21,22], a phenomenon that has been exploited in alkanethiol UV photopatterning [23]. In the attempt to combine the techniques of hydrogel photocrosslinking and SAM electrochemical cell patterning, it is therefore essential to characterize the possible effects of UV irradiation in the presence of PI (PI&UV) on SAM.

To assess the effect of PI&UV on SAM removal, oligopeptide modified substrates were exposed to UV in PI solution (in the absence of GelMA prepolymer) at the same conditions adopted for hydrogel photopolymerization. SAM stability was investigated with QCM mass adsorption/desorption and XPS surface chemistry analyses. QCM analysis showed that the resonant frequency of bare gold sensors (Fig. 2A.I) decreased after being immersed in the oligopeptide solution (Fig. 2A II-III) as a result of SAM adsorption on the surface [7]. When the oligopeptide modified substrate was exposed to PI&UV, the resonant frequency increased, and the initial shift was partially reduced (28.0 ± 5.1%) (Fig. 2A.IV), indicating a loss of the adsorbed mass from the gold surface. Also XPS analysis revealed a change in the surface chemistry of SAM modified gold substrates exposed to PI&UV. Spectrum peaks of peptide constituents such as carbon, oxygen, and nitrogen decreased compared to the controls rinsed in PBS (Fig. 2B), with a calculated loss of surface mass concentration of 22.7% (carbon), 13.8% (oxygen), and 3.2% (nitrogen). These observations suggest that UV irradiation in the presence of PI can affect oligopeptide SAM coating on gold substrates, resulting in a partial desorption of the adsorbed peptides. Previous studies on UV effects on alkanethiol molecule have identified photo-oxidation of the S-Au bond as the major reason for SAM desorption, but the exact mechanism is still not clear [24,25]. Other bond scissions (such as C-S bond) have also been indicated to contribute to the process [26]. However, since our experimental conditions differ from previously reported studies, SAM desorption might have occurred via alternative mechanisms.

To evaluate the influence of photoinitiated SAM desorption on cell adhesion, HUVECs were seeded at a low density (15.6×10^3 cells/cm^2) on gold surfaces. Cells readily adhered (sparse adherent cell population with negligible cell–cell contact) and acquired a spread morphology (Fig. 2D). After 16 h, substrates were irradiated with UV in a PI solution without GelMA prepolymer (PI concentration and UV exposure identical to those used for GelMA photopolymerization). Analysis of phase contrast images taken before and after PI&UV exposure show a significantly decreased cell population (71.9 ± 3.4%) on SAM modified gold substrates characterized by a rounded morphology (Fig. 2C,E). When submerged in PBS in the absence of PI&UV, cells remained adherent and maintained a spread morphology (Fig. 2C,F) supporting the role of PI&UV in the detachment process. Finally, cells cultured on non-modified substrates did not detach or change morphology when exposed to PI&UV (Fig. 2G). These results indicate that cell detachment and morphology rearrangement originate from the interactions among peptide, PI, and UV, rather than from peptide-independent mechanisms such as a cytotoxic effect of PI and UV.

Together these findings confirm that PI&UV, crucial to hydrogel photopolymerization, are involved in the partial desorption of SAM. Our results suggest also that this process leads to the loss of oligopeptide-mediated cell adhesion sites, resulting in a more rounded cell morphology and partial cell detachment. This phenomenon could constitute a mechanism additional to electrochemical SAM desorption, contributing to cell transfer to the hydrogel.

3.2. Cell transfer

To probe cell transfer from modified and non-modified gold substrates to GelMA hydrogels with and without electrochemical SAM desorption, HUVECs were seeded on both modified and non-modified gold surfaces for 16 h. Cells adhered to the surface and spread in a similar fashion (Fig. 3A–C) under both conditions. After photocrosslinking GelMA solution on HUVECs, an electrical potential (−1.0 V, 2 min) was applied to non-modified (Pep^- El^+) and modified (Pep^+ El^+) samples before removing the hydrogel.

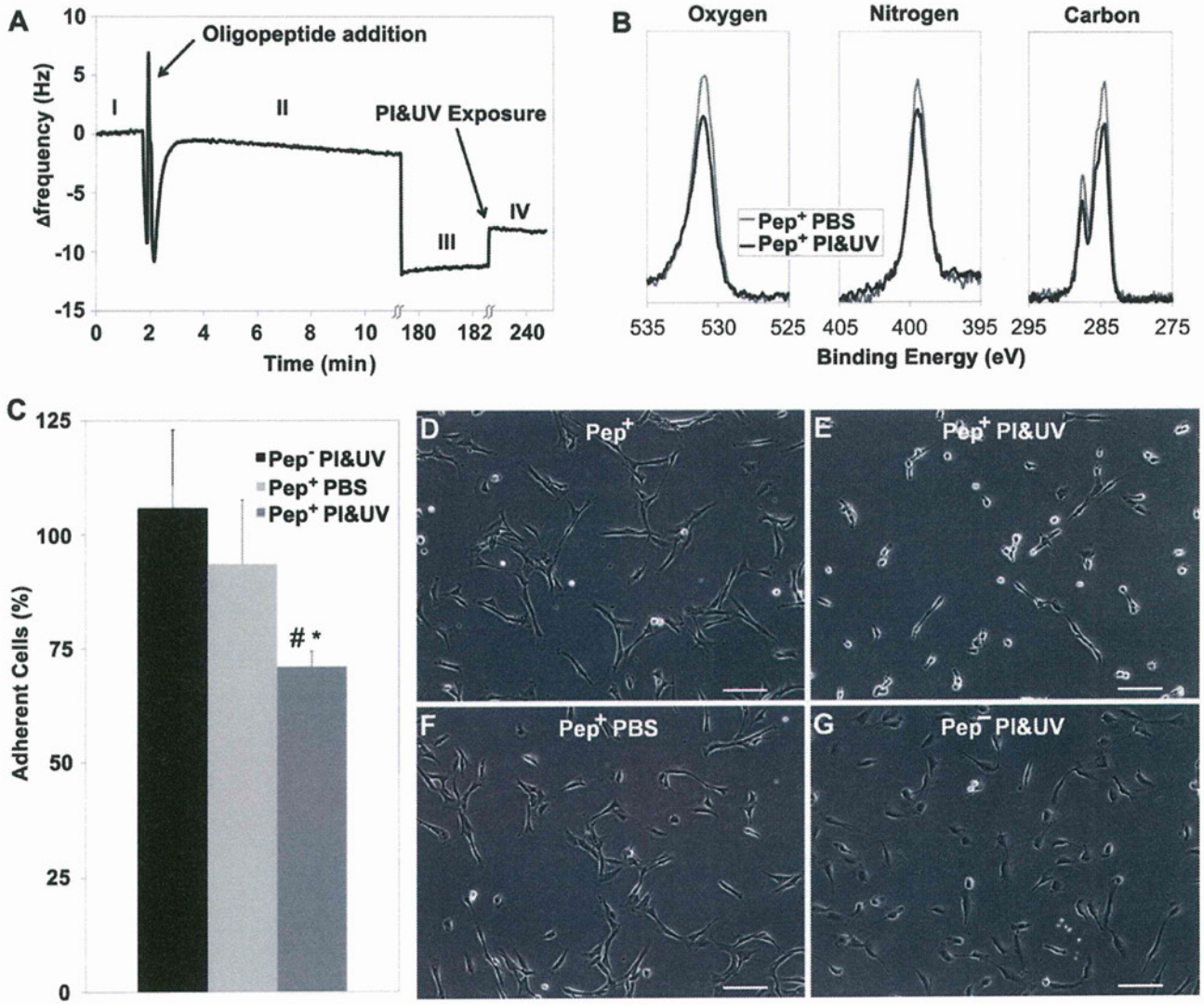

Fig. 2. Effect of PI&UV on the removal of SAM and HUVEC adhesion. (A) Resonant frequency of bare gold surface (I) decreased with oligopeptide adsorption over time (II, 10 min; III, 180 min), and increased after PI&UV exposure, due to mass desorption (IV). (B) XPS surface analyses show decreased oxygen, nitrogen and carbon peaks after PI&UV exposure. (C) Percentage of adherent HUVECs on modified substrates upon exposure to PI&UV (Pep^+ PI&UV) show almost 30% cell detachment as compared to non-modified substrates (Pep^- PI&UV) or modified substrates exposed to PBS (Pep^+ PBS). Representative phase contrast images show that HUVECs adhering on modified substrates (D) acquire a rounded morphology after PI&UV (E). The cells maintained a spread morphology on modified substrates when exposed to PBS (F) or on non-modified substrates when exposed to PI&UV (G). PI&UV exposure induce loss of fraction of the adsorbed SAM leading to partial cell detachment. (Scale bars: 100 μm; error bars: ± SD; statistically significant difference from Pep^+ PBS # and Pep^- PI&UV *).

A third group was prepared with modified samples without electrical potential application (Pep^+ EI^-). Images of the gold surfaces after GelMA removal (Fig. 3D–F) show that most of the cells still adhered to the non-modified gold surface (Fig. 3D), but only a negligible number of cells remained on the modified gold surfaces regardless of the potential application (Fig. 3E,F). Images of the hydrogel after transfer (Fig. 3G–I) show that only 20% of the cells on the non-modified gold surface were transferred to the hydrogel (Fig. 3J). More than 50% of these cells were stained by EthD-1 (Fig. 3K) 2 h after transfer. Both the transfer efficiency and the viability were significantly higher for the surfaces modified with the SAM. Indeed, regardless of whether the potential was applied, almost 100% of the cells were transferred to the GelMA constructs (Fig. 3J) and more than 90% of the cells were viable after 2 h. Samples without electrical potential application presented slightly lower but not statistically different viability (Fig. 3K). These results underline the importance of the oligopeptide modification process for efficient cell transfer.

To explore the effect of oligopeptide electrochemical cleavage on cell morphology, fluorescent images of the cells seeded on the gold surfaces were analyzed to quantify the mean cell area and its distribution (Fig. 4A,B). The few cells transferred from substrates without oligopeptide modification presented mostly a rounded morphology (Fig. 3G) and a mean area significantly lower than those from the modified substrates (Fig. 4A). For the modified substrates, the electrochemical cleavage of the SAM resulted in a significantly higher mean cell area compared to cells transferred without potential, and an overall cell area distribution closely resembling the one on gold substrates (Fig. 4B) before cell transfer. In addition, the cells transferred with potential application presented a statistically higher percentage of spread cells after 12-h culture (Fig. 4C–E), but no significant difference was observed in terms of proliferation and viability at 72-h culture. Indeed, regardless of electrochemical oligopeptide desorption, the cells proliferated on the hydrogel for 3 days, displaying viability close to 100% (Fig. 4C,F) after 72 h.

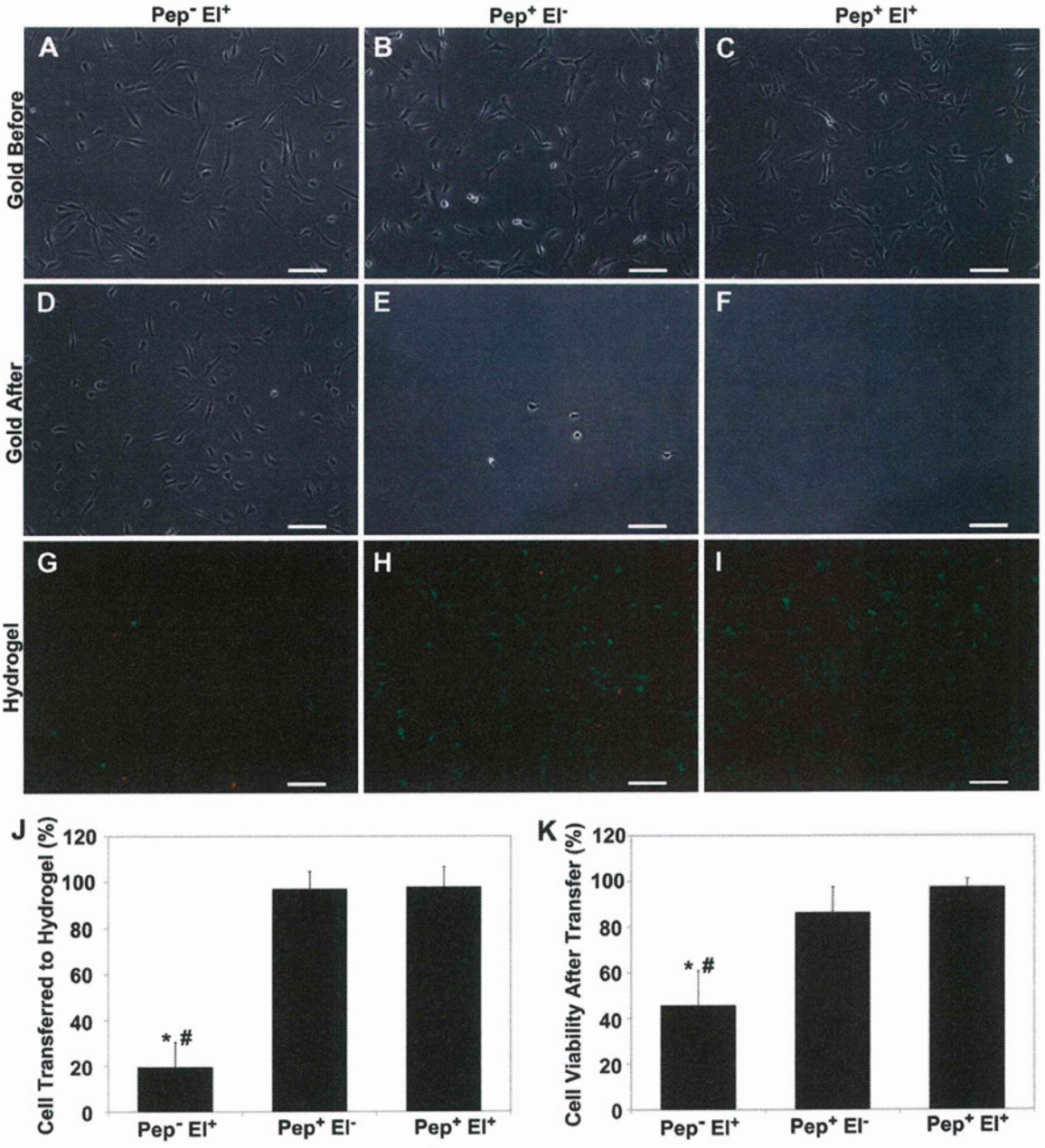

Fig. 3. Cell transfer from gold substrate to hydrogel. Cells were transferred from non-modified substrates with electrical potential (Pep^{-} El^{+}), modified substrates without electrical potential (Pep^{+} El^{-}), and modified substrate with electrical potential (Pep^{+} El^{+}). Representative phase contrast images of the same substrate before (A–C) and after (D–E) transfer show negligible number of cells still adherent on peptide coated gold after transfer as opposed to the high number of cells on non-modified substrates. The corresponding fluorescent images (GFP/EthD-1) of the hydrogels after transfer display few rounded cells for the Pep^{-} El^{+} (G) and numerous viable spread HUVECs for both Pep^{+} El^{-} (H) and Pep^{+} El^{+} (I). (J) Mean percentage of cell transferred to hydrogel confirms that peptide modification enables complete HUVEC transfer as compared to only 20% of cells for Pep^{-} El^{+}. (K) Mean cell viability after transfer similarly illustrates that both modified substrates promoted transfer with high cell viability as opposed to non-modified ones (less than 50% viable cells). Gold surface coating with oligopeptide SAM enables HUVEC transfer to GelMA hydrogels with high efficiency and viability independent of electrochemical SAM desorption. (Scale bars: 100 μm; error bars: ± SD; statistically significant difference from Pep^{+} El^{-} # and Pep^{+} El^{+} *). (For interpretation of the references to colour in this figure legend, the reader is referred to the web version of this article.)

Cell transfer is achieved when the cells detach from a substrate and adhere to a new substrate. Previous studies on electrochemically desorbed SAM indicate that cell detachment occurs in two steps: externally triggered cleavage of cell-substrate adhesion sites, followed by an active metabolic driven rearrangement of the cytoskeleton [27]. A similar process has been proposed for thermoresponsive substrates [28], while final cell removal from the substrate has been shown to be dependent on external forces such as those generated by fluid flow or cell–cell interactions [29,30]. In fact, cell detachment from a substrate and transfer to a new one depends on the balance of interaction forces between cells and each substrate. Recently, Weder *et al.* have quantitatively demonstrated that triggered cell detachment and consequent decreased cell-surface adhesion are crucial to highly efficient cell transfer to a new substrate [31].

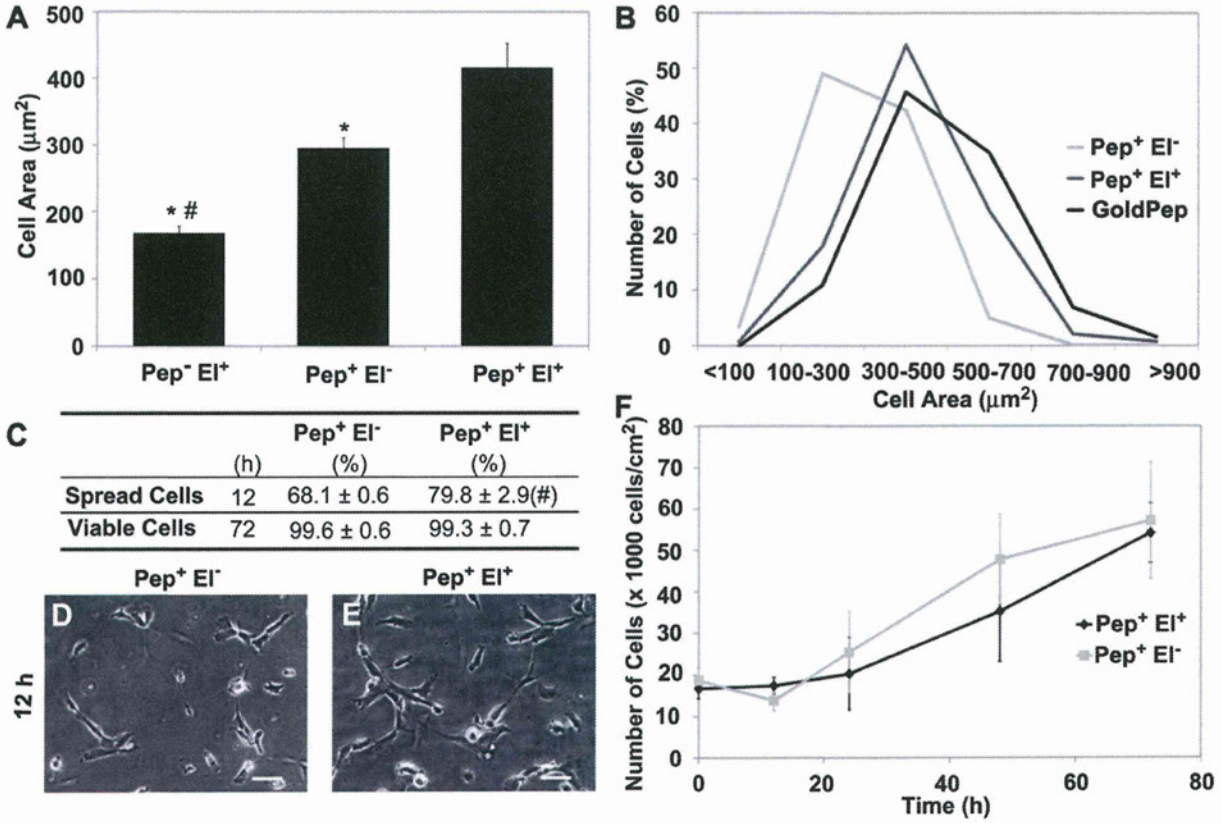

Fig. 4. Cell morphology and proliferation upon transfer. (A) Mean cell area after transfer shows that $Pep^- El^+$ cells occupy significantly smaller area than $Pep^+ El^-$ and $Pep^+ El^+$, the latter being statistically more spread among the modified substrates. (B) Cell area distribution shows that cells transferred from the modified substrates using potential ($Pep^+ El^+$) maintained a similar morphology whereas those transferred without potential ($Pep^+ El^-$) tended to be less spread than on gold substrates. (C) Similarly, a higher percentage (Mean ± SD) of cells (E) presented a spread morphology at 12 h on $Pep^+ El^+$ hydrogels compared to cells on $Pep^+ El^-$ (D). However, electrochemical oligopeptide cleavage did not show significant effect on the percentage (Mean ± SD) of viable cells (C) and on proliferation (F) after transfer. While electrochemical SAM desorption has an effect on the cell morphology immediately after transfer, no differences are evidenced on longer cultures both conditions maintaining proliferative cell population. (Scale bars: 50 μm; error bars: ±SD; statistically significant difference from $Pep^+ El^-$ # and $Pep^- El^+$ *).

In our system, cell transfer occurs when cell-hydrogel interaction forces are greater than cell-gold adhesion forces. When cells adhere to the substrate through non-specifically adsorbed proteins ($Pep^- El^+$), the balance favors cell-gold interactions. Few cells are transferred, and a considerable fraction of the transferred cells presents a compromised membrane, most likely due to mechanical stress as cells are peeled off from the substrate [32]. As the electrical potential is applied on the modified substrate, the gold-thiol bond is reductively cleaved, dramatically reducing cell adhesion, therefore promoting a highly efficient transfer of the cells to the hydrogel with negligible effect on cell viability. Surprisingly, our results pointed out that even in the absence of electrochemical thiol-gold cleavage ($Pep^+ El^-$) the force balance favors cell transfer, with efficiency and viability similar to those obtained with potential application. This finding appears to be consistent with our observations about the UV mediated SAM desorption in PI solution and the consequent partial cell detachment.

Cell transferred to the hydrogel displayed a spread morphology, suggesting that the rapid onset of cell-hydrogel interaction points provides sufficient adhesion sites for maintaining cell area during the transfer. The different cell area after transfer with or without potential may be caused by distinctive residual cell-gold adhesion forces rather than a difference in cell-hydrogel adhesion. Indeed, although electrochemical oligopeptide cleavage was shown to induce almost complete cell detachment [7], only 30% of cells came off with photoinduced SAM desorption (Fig. 2C). The remaining population retained a number of adhesion sites with the gold that could act as traction points during the peeling process, contributing to cell deformation and eventually loss of cell spreading [33,34]. The dismissal of electrochemical oligopeptide desorption also led to a slightly lower spread population at 12-h culture but did not affect proliferation and viability over 3 days (Fig. 4C,F).

Overall, these results suggest that the electrochemical SAM desorption step influences the degree of dissociation of cell-gold adhesion sites, which affects the mechanics of cell transfer and therefore the initial cell morphology and spreading. Nevertheless, regardless of potential application, cell transfer from oligopeptide-SAM coated gold substrates to hydrogel is highly efficient and preserves both cell viability and proliferation ability.

3.3. Cell monolayer transfer

HUVEC monolayer transfer from oligopeptide modified substrates to hydrogel was investigated by seeding the cells at a low density (15.6×10^3 cells/cm^2) and culturing them for 72 h (LD-72 h), or by seeding at a high density (10.4×10^4 cells/cm^2) and culturing for 16 h (HD-16 h). In both conditions, confluent cell monolayers were obtained by the end of the culture period with similar cell numbers ($10.26 \pm 0.60 \times 10^4$ cells/cm^2). After hydrogel photocrosslinking, samples were transferred either with ($Pep^+ El^+$) or without ($Pep^+ El^-$) electrical potential (−1.0 V, 2 min). The results for the HD-16 h samples were similar to those obtained with

sparse cells. The entire cell population was transferred to the hydrogel regardless of electrochemical oligopeptide desorption and a continuous cell monolayer covering the hydrogel surface (Fig. 5A,B,E) was obtained. The LD-72 h samples displayed lower transfer efficiencies than the HD-16 h samples, with significant differences between Pep^+ El^- and Pep^+ El^+ (Fig. 5C,D). Without electrochemical SAM desorption, only 32.9 ± 16.4% of the cells were transferred, whereas a significantly higher efficiency was obtained with electrochemical SAM desorption, successfully transferring 80.9 ± 6.5% of the cells (Fig. 5E). The fraction of HUVECs remaining on the gold substrate suggests that the effect of culture period on transfer efficiency was most likely due to a shift in the hydrogel-cell/cell-gold force balance toward gold.

Whereas cell-gold adhesion forces increase during the first cell spreading and cytoskeleton rearrangement [35], the onset and maturation of cell–cell interactions at later time points have been correlated with decreased cell-substrate interactions [36]. This process has been shown to eventually sustain the cell transfer [37].

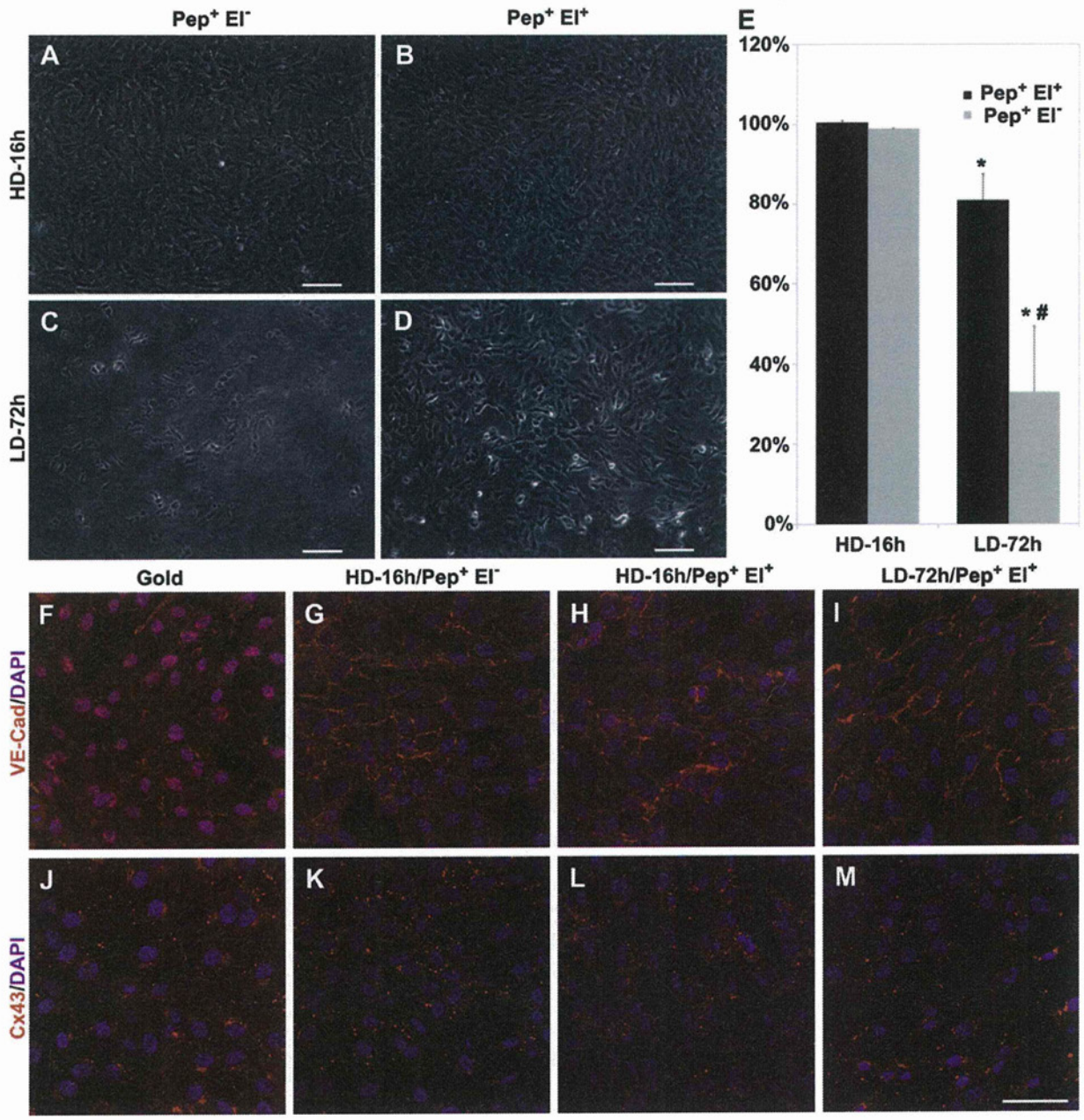

Fig. 5. HUVEC monolayer transfer. Representative phase contrast images of hydrogels after transfer from modified substrates seeded at high density and cultured for 16 h (HD-16 h) (A,B) or at low density and cultured for 72 h (LD-72 h) (C,D) transferred either without (A,C) or with (B,D) potential (Scale bars:100 μm). (E) Mean percentage of cells transferred to hydrogel decreases upon longer culture, maintaining however high transfer efficiency (over 80%) when SAM was electrochemically desorbed (Pep^+ El^+). (F–M) Representative confocal images of gold and hydrogel samples show intact VE-Cad junctions while Cx43 is mostly internalized upon transfer. Both processes were not affected by transfer method and culture period on gold. Although endothelial monolayers can be transferred both with and without electrical potential, the longer culture requires electrochemical oligopeptide cleavage for efficient transfer (Scale bars: 50 μm). (Error bars: ± SD; statistically significant difference between culture period * and between transfer protocol #). (For interpretation of the references to colour in this figure legend, the reader is referred to the web version of this article.)

Nonetheless, a longer culture time exposes SAM to a greater chance of contamination by proteins from the medium or secreted by the cells [38]. These proteins would behave as non-cleavable anchoring sites that increase cell-gold residual interaction forces, which eventually hinder cell transfer. The effect of these contaminants is expected to be more dramatic without electrochemical SAM desorption since photoinduced oligopeptide desorption has been shown to be only partial, and therefore have constitutively higher residual adhesion forces.

While investigating endothelial monolayer transfer, it is crucial to evaluate the effect of transfer process on cell–cell junctions, a class of proteins vital to monolayer functions. Among the other junctions, VE-Cad adherens junction and Cx43 gap junction play fundamental roles in regulating vascular stability and selective permeability to molecules and cells [39,40]. To investigate the effect of cell transfer on cell–cell junctions, all HD-16 h and LD-72 h samples, with the exception of LD-72 h Pep^+ El^-, were fixed and stained for VE-Cad and Cx43 before and 2 h after transfer. On gold substrates, the endothelial monolayer exhibited positive VE-Cad staining at cell–cell boundaries (Fig. 5F), confirming the characteristic onset of endothelial monolayer cell–cell junctions for cells cultured on SAM. On the hydrogel, the monolayer still presented a clear VE-Cad positive staining at the cell–cell edges, suggesting that the adherens junctions were preserved over the transfer process both without and with electrochemical desorption at HD-16 h (Fig. 5G,H) and for LD-72 h when the potential was applied (Pep^+ El^+, Fig. 5I). On the contrary, Cx43, which on gold was mostly restricted to cell–cell boundaries (Fig. 5J), after transfer displaced from the periphery to the inner compartment of cells, often in proximity to the cell nuclei (Fig. 5K–M). This rearrangement, which occurred independently from the transfer condition, is typical of connexin internalization. This process was shown to be transiently increased by UV exposure, peaking at 2 h and returning to baseline values after 8 h [41], as part of the gap junction dynamic synthesis-proteolysis [42].

Although previous studies have described successful applications of endothelial cell transfer in tissue engineering [37,43,44], their approaches mostly depend on active cell migration, a process that required significantly longer transfer time (up to 24 h) and a meticulous design for cell relative binding affinity to initial and receiving substrates. The introduction of a triggered detachment process enables a controlled transfer of the endothelial cell monolayer from oligopeptide coated gold substrate to photo-crosslinkable GelMA within few minutes. High efficiency can be obtained relying either on a photoinduced partial SAM desorption or on its combination with electrochemical oligopeptide cleavage. While the photoinduced mechanism alone eliminates the need for electrical connections and equipment, our results established that the combination of photo- and electrical SAM desorption preserves higher cell transfer efficiency over time. Besides this, both approaches were shown to conserve VE-Cad junctions, critical to cell–cell communication, monolayer maturation, vascular generation and physiological functions. Considering the central role of cell–cell junctions in vascular function, further studies are needed to evaluate the junction rearrangement, focusing specifically on Cx43, a highly dynamic junction, which was currently shown to be disrupted during the cell transfer process.

3.4. Microvascular structure generation

After characterizing the transfer process on 2D substrate, the combination of SAM-based cell transfer and hydrogel photopatterning was investigated in a more complex 3D setting as a platform for rapidly engineering *in vitro* vessels, featuring a readily available hollow structure and controlled geometrical design. Gold sputtered rods, with a diameter of 600 μm, were modified with the oligopeptide, seeded with HUVECs and then cultured in petri dishes (3–4 days) until uniformly covered by a confluent endothelial monolayer (Fig. 6A). Based on the previously described results concerning the effect of culture time on cell transfer, after GelMA photocrosslinking, we applied a −1.0 V potential to achieve optimal HUVECs transfer. Following the removal of the rod, tubular structures completely lined with an endothelial monolayer were obtained, having a length of 10 mm and a diameter of 618 ± 15 μm (Fig. 6B). The geometry of the channels was stable as no deformations or shrinkages were observed following the fabrication process. Mimicking *in vivo* conditions, cultured samples were maintained under perfusion for up to 15 days. Confocal images acquired at 12 h show that HUVECs displayed a spread morphology and covered the inner surface of the channel with no particular signs of cell detachment or wash out (Fig. 6C), thus suggesting sufficient construct oxygenation and the absence of detrimental effects of toxic photopolymerization residues. Representative images of construct sections show a cell monolayer lining on the inner surface of the channel (Fig. 6D), accurately replicating the circular cross-section of the rod and mimicking the arrangement of endothelial cells *in vivo*, while volumetric reconstructions illustrate the hollow tubular cell monolayer (Fig. 6E). Images after 5 days of culture show a compact cell population completely lining the hydrogel surface (Fig. 6F). The constructs maintained a stable geometry over the 15-day culture with no evidence of channel deformation due to hydrogel collapse or cell layer detachment. Indeed, even after 15 days of culture the engineered vascular structure displayed a hollow channel encircled by cells (Fig. 6G). In contrast to our previous experiments with collagen [7] cells did not invade the hydrogel even at the latest time points. Due to the absence of cell–cell contact proliferation inhibition, typical of immortalized cell line, the HUVECs were rather prone to grow into a multicellular endothelial layer.

To investigate if the proposed hydrogel photopatterning could be adapted to microengineer *in vitro* the complex multilayered geometrical organization of blood vessels, double-layer cell constructs were generated by adding a cell-laden hydrogel stratum encircling the endothelial monolayer. Adopting a dip-coating approach, namely the immersion/withdrawal of HUVEC confluent gold rods in a 3T3 cell-GelMA prepolymer suspension, cell suspension was conveyed onto the rod surface, obtaining uniform second cell layers that were immediately photocrosslinked (Fig. 6H). The thickness of the deposited layer, in a dip-coating approach, is known to be primarily determined by fluid viscosity, which in our case mainly depends on prepolymer concentration and solution temperature, adjusted in our experiments to obtain a thickness of one to three cells. The double-layer constructs were embedded in hydrogel as previously described. After potential application and rod removal, channels with an outer 3T3-cell layer (Fig. 6I) lined with an inner HUVEC monolayer (Fig. 6J) were obtained. The composed image of the two layers shows that the external layer creates a homogeneous cellular frame (one to three cell thick) in close geometrical proximity with the endothelial layer (evidenced also by partial fluorescence overlap) (Fig. 6K). This organization mimics well the structural arrangement of distal arterioles, characterized *in vivo* by an endothelial monolayer encircled by one to two layers of smooth muscle cells.

As previously mentioned, current approaches for generation of vascular structures suffer from several limitations such as the lack of control on 3D tubular organization and the extensive culture time required for the arrangement of endothelial cell monolayer into patent vascular structures [1,5]. Our results show that the combination of hydrogel photopolymerization and SAM-based cell transfer dramatically shortens the process to generate *in vitro*

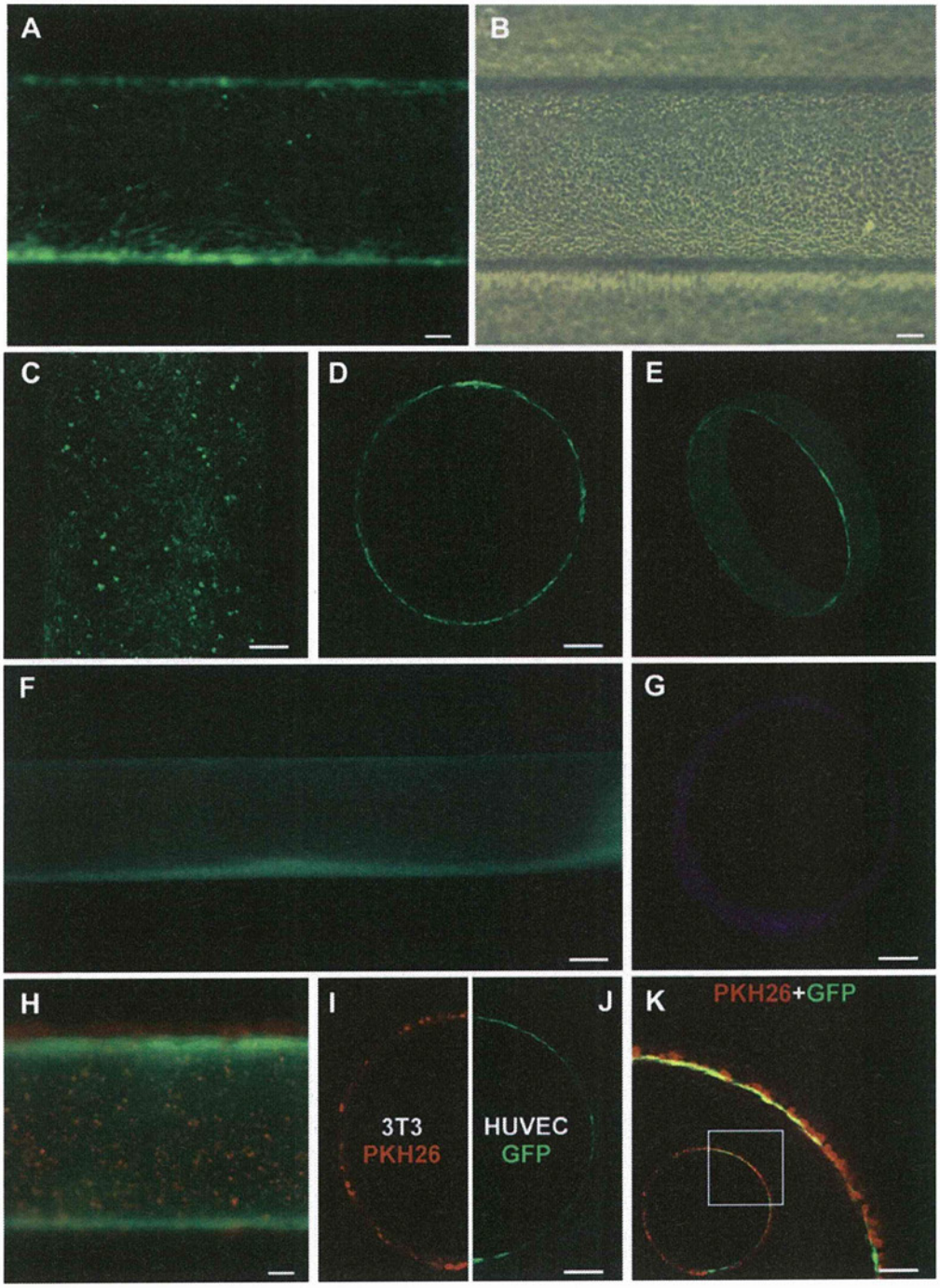

Fig. 6. Fabrication of microvascular-like structures. (A) HUVECs were cultured on gold rods for three days to create a confluent monolayer. (B) After GelMA photocrosslinking, electrical potential application and rod removal, HUVECs were transferred uniformly on the hydrogel channel surface. (C) The constructs, cultured under perfusion, maintained a continuous endothelial monolayer lining the surface of the channel (D) mimicking the 3D endothelial cell organization in microvasculature (E). (F) Over 5 days of culture, the constructs maintained a stable shape and a compact cell layer on the channel surface. (G) After 15 days of culture, samples stained with DAPI and cross-sectioned displayed a hollow channel structure that was maintained over long term culture. (H) GelMA encapsulated PKH26-stained 3T3 cells photopatterned on HUVEC monolayer seeded on gold rods. (I) Confocal image showing cross-section of hydrogel channel covered with 3T3 cells, (J) lined with HUVEC monolayer. (K) Magnified merged confocal image shows both 3T3 (PKH26) and HUVEC (GFP) layer patterned in close proximity (inset shows the entire channel section). (All scale bars: 100 μm, except F: 200 μm, and K: 50 μm). (For interpretation of the references to colour in this figure legend, the reader is referred to the web version of this article.)

vascular-like structures lined with endothelial cell monolayers. Moreover, the proposed method provides a precise and stable geometrical outline of vascular structures. This crucial attribute determines fluid dynamic conditions, critical to vascular construct designed for *in vitro* models [45,46] as well as for *in vivo* applications [47]. Furthermore, the conjunction of rapid polymerization with high geometrical control paves the way to the design of more challenging 3D vascular architectures. As a proof of concept, the photopatterning was extended to the generation of double-layer constructs, demonstrating that the approach could